Microscopic analysis of the crystal field strength and electron-vibrational interaction in cubic $SrTiO_3$ doped with Cr^{3+}, Mn^{4+} and Fe^{5+} ions

2009 J. Phys.: Condens. Matter 21 155502

(http://iopscience.iop.org/0953-8984/21/15/155502)

J. Phys.: Condens. Matter **21** (2009) 155502 (9pp) doi:10.1088/0953-8984/21/15/155502

Microscopic analysis of the crystal field strength and electron-vibrational interaction in cubic $SrTiO_3$ doped with Cr^{3+}, Mn^{4+} and Fe^{5+} ions

M G Brik[1,4] **and N M Avram**[2,3]

[1] Institute of Physics, University of Tartu, Riia 142, Tartu 51014, Estonia
[2] Department of Physics, West University of Timisoara, Boulevard V Parvan 4, 300223 Timisoara, Romania
[3] Academy of Romanian Scientists, Independentei 54, 050094 Bucharest, Romania

E-mail: brik@fi.tartu.ee

Received 13 January 2009, in final form 25 February 2009
Published 20 March 2009
Online at stacks.iop.org/JPhysCM/21/155502

Abstract

A detailed microscopic study of the crystal field strength $10Dq$ for different interionic distances in cubic $SrTiO_3$ doped with three isoelectronic ions (Cr^{3+}, Mn^{4+} and Fe^{5+}) was performed. The exchange charge model of the crystal field was used to calculate the $10Dq$ values at different distances between impurity ions and ligands. The obtained results were represented by the power laws $1/R^n$, with $n = 4.9050$, 5.7990 and 6.5497 for Cr^{3+}, Mn^{4+} and Fe^{5+}, respectively. For the first time the role of two different contributions (the point charge and exchange charge) into the total crystal field strength was studied separately. With the obtained $10Dq(R)$ dependences, a number of important physical quantities describing the optical and dynamical properties of impurity centers (such as the constants of the electron-vibrational interaction, Huang–Rhys parameters, Stokes' shifts, Jahn–Teller stabilization energies, changes of the chemical bond lengths due to the combined effect of the local vibrational normal modes, bulk modulus and Grüneisen constants for the a_{1g} normal mode) were calculated. The obtained results are in good agreement with available experimental data and can be readily applied for analysis of the optical spectra, electron-vibrational interaction and pressure effects for these and other similar systems.

(Some figures in this article are in colour only in the electronic version)

1. Introduction

Energy levels of any impurity ion with unfilled electron shells can be split by an external electric or magnetic field. A very common and widely used situation is when such an ion is located inside a crystal or a glass (no matter whether it intrinsically belongs to this material or was incorporated into it artificially). In this case the electrostatic field created by other surrounding ions is referred to as a crystal field (CF) and the overall splitting pattern of the impurity ion energy levels depends simultaneously on several factors, among which one can mention electrical charges of the impurity ion and surrounding ions, interionic separation, symmetry of an environment around impurity, exchange and overlap interactions between impurity ion and its neighbors, etc [1–4]. It is common practice to use for the cubic crystal fields (for the O_h, T_d ideal symmetries or for very small deviations from a perfect symmetry) a single parameter—the so-called cubic CF strength $10Dq$—to describe the possible variations of the CF and distinguish between different special cases. This parameter is used when considering the energy levels of ions with unfilled d-electron shells. It is defined as the energy interval between the antibonding e_g and t_{2g} orbitals of the central ion [1] (where e_g and t_{2g} indicate the symmetry properties of the wavefunctions of the split states transforming

[4] Author to whom any correspondence should be addressed.

according to the corresponding irreducible representations of the O_h point group). In this form the above definition can be used only when working with CF of an ideal cubic symmetry; it should be kept in mind that the CF of lower symmetries splits further the e_g and t_{2g} states and one should then follow the positions of the barycenters of the split levels.

It is a straightforward procedure to show in the framework of the simplest point charge model of CF [1] that $10Dq$ depends on the interionic separation R as $1/R^n, n = 5$. However, already soon after the pioneering works of Sugano and Tanabe [5, 6] it was firmly established that the estimation of $10Dq$ predicted by the point charge model is several times smaller than the corresponding experimental values, which is a clear indication that the value of n is different from 5. More elaborate models based on molecular orbital calculations and DFT theory, which extend their area of applicability far beyond the point charge model limits, have led to values of n in a rather wide interval from 3.5 to 7.3 for different systems [7–12]. Such a wide range shows that behavior of the CF strength $10Dq$ is very much sensitive to the impurity ion environment and cannot be easily transferred from one system to another. It is very attractive to know exactly how $10Dq$ depends on the distance between impurity ion and ligands, since such knowledge can help in getting valuable information about essential electronic properties of an impurity center in a crystalline host, such as the constants of electron-vibrational interaction (EVI), energetic Stokes' shifts (differences between the maxima of the first absorption and emission bands), Huang–Rhys parameters, compressibility, Grüneisen parameters, etc [7, 9, 10]. An additional motivation for such studies (both experimental and theoretical) is that the high-pressure experiments with various doped materials [13–15] show that an external pressure (which eventually changes the interionic distances) can significantly affect the optical properties of a considered system, giving an opportunity to adjust the positions of the absorption and emission bands to particular purposes. The results of these high-pressure measurements can serve as a reliable test for the theoretical calculations. Therefore, a thorough microscopic (in a sense that the small variation of the ionic positions should be considered) analysis of the $10Dq(R)$ dependence for a number of impurity ions in various hosts is an important and interesting task.

Among the recently published theoretical works on this subject we mention the first-principles-based analysis of the $10Dq$ and charge transfer transitions for the Cr^{3+} in Cs_2NaYF_6, Cs_2NaYCl_6 and Cs_2NaYBr_6 [16], pressure effects for the Cr^{3+} ions in $Cs_2NaScCl_6$ and Cs_2NaYCl_6 [17], determination of the different origin of colors of $MgAl_2O_4$ and $Be_3Si_6Al_2O_{18}$ doped with Cr^{3+} [18], consideration of properties of the chemical bonds between Fe^{3+} and ligands in $KMgF_3$ [19], etc. In all these publications the DFT-based *ab initio* methods were successfully applied.

However, it should be pointed out that such calculations are rather complicated, and an increase in the calculations' accuracy can be achieved on account of an increase of the computational time. From this point of view, the problem of development of a simple semi-empirical approach with as small a number of fitting parameters as possible, which can be easily applied to the microscopic studies of the CF effects to get reasonable results, remains important.

In an attempt to fill this gap, in this paper we present a semi-empirical analysis of the dependence of CF strength parameter $10Dq$ on the interionic distance for three isoelectronic ions (Cr^{3+}, Mn^{4+} and Fe^{5+}; all having three d electrons in the 3d shell) in cubic $SrTiO_3$. The calculations were performed in the framework of the exchange charge model (ECM) of CF [20] using the Stevens normalization for the CF parameters (CFP). The functional dependences of $10Dq$ on the distance between impurity ion and ligands were obtained and used for estimation of the EVI constants, Huang–Rhys factors, Jahn–Teller stabilization energies, bulk modulus, compressibility and Grüneisen parameters.

The choice of the cubic strontium titanate is determined by high symmetry (O_h) of the Ti^{4+} position, which is occupied by impurities. In addition, $SrTiO_3$ with different dopants is an intensively studied host with numerous potential applications [21–26].

The structure of this paper is as follows. In section 2 we briefly describe the main ideas underlying the calculation method. Then we proceed with a short summary of the crystal structure and optical data for the considered systems, present the obtained results and, after discussion, conclude the paper with a brief summary.

2. Method of calculations

The energy levels of impurities with unfilled d shells in crystals can be represented as the eigenvalues of the following CF Hamiltonian:

$$H = \sum_{p=2,4} \sum_{k=-p}^{p} B_p^k O_p^k, \tag{1}$$

where O_p^k are the suitably chosen linear combinations of the irreducible tensor operators acting on the angular parts of the impurity ion's wavefunctions and B_p^k are the CFP, which include all the structural and geometrical information about the considered host. In the ECM model the CFP are written as a sum of two terms [20]:

$$B_p^k = B_{p,q}^k + B_{p,S}^k. \tag{2}$$

where

$$B_{p,q}^k = -K_p^k e^2 \langle r^p \rangle \sum_i q_i \frac{V_p^k(\theta_i, \varphi_i)}{R_i^{p+1}}, \tag{3}$$

is the point charge contribution to the CFP which represents the electrostatic interaction between the central ion and the lattice ions i with charges q_i and spherical coordinates R_i, θ_i, φ_i. The mean values $\langle r^p \rangle$, where r is the radial coordinate of the d electrons of the impurity ion, can be either taken from the literature or calculated numerically, using the corresponding ion's wavefunctions. The values of the numerical factors K_p^k and expressions for the polynomials V_p^k along with the definitions of the operators O_p^k can be found in [20]. The second term of equation (2) is proportional to the overlap between the wavefunctions of the central ion and ligands and

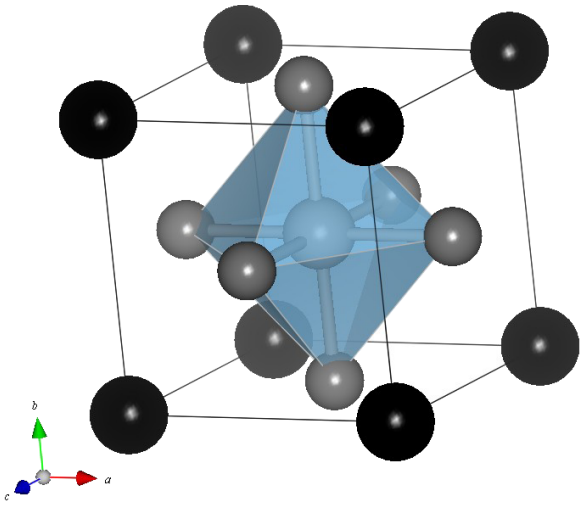

Figure 1. Crystal structure of $SrTiO_3$. One unit cell is shown in the figure; Sr^{2+} ions are at the corners of the cube; Ti^{4+} ion is at the center of the oxygen octahedron.

thus includes all covalent effects. It can be calculated using the following formula:

$$B^k_{p,S} = K^k_p e^2 \frac{2(2p+1)}{5} \sum_i \left(G_s S(s)_i^2 + G_\sigma S(\sigma)_i^2 + \gamma_p G_\pi S(\pi)_i^2\right) \frac{V^k_p(\theta_i, \varphi_i)}{R_i}. \quad (4)$$

$S(s)$, $S(\sigma)$, $S(\pi)$ correspond to the overlap integrals between the d functions of the central ion and the p and s functions of the ligands: $S(s) = \langle d0|s0\rangle$, $S(\sigma) = \langle d0|p0\rangle$, $S(\pi) = \langle d1|p1\rangle$. The numerical constants γ_p, which depend on the quantum numbers of the overlapping wavefunctions, are also given in [20]. G_s, G_σ, G_π are dimensionless adjustable parameters of the model, whose values are determined from the positions of the first three absorption bands in the experimental spectrum. We assume that they can be approximated to a single value, i.e. $G_s = G_\sigma = G_\pi = G$, that can be estimated from only one absorption band. This is usually a reasonable approximation [20].

One of the advantages of the ECM is that it not only allows for reliable calculations of the energy levels of impurities in crystals, but also for a quantitative treatment of the covalent effects (by calculating the overlap integrals) and analysis of the EVI parameters (by direct differentiation of the expressions for the CFP with respect to the ligand's displacements).

3. Crystal structure and spectroscopy for $SrTiO_3$ doped with Cr^{3+}, Mn^{4+}, Fe^{5+} ions

$SrTiO_3$ crystallizes in a perovskite-type structure, space group $Pm3m$ and lattice constant $a = 3.905\,28$ Å [27]. After doping, Cr^{3+} (Mn^{4+}, Fe^{5+}) substitute for the Ti^{4+} ion at the center of the oxygen octahedron (figure 1). The Ti^{4+}–O^{2-} distance is 1.9526 Å [27].

Although the optical properties of these three ions in $SrTiO_3$ were studied previously [21, 22, 28–33], the main spectroscopic parameters (the Racah parameters B and C along with the CF strength $10Dq$) reported in the literature are somewhat different (table 1). For example, the Racah parameter B and crystal field strength Dq for Cr^{3+} in [28] were estimated (in cm^{-1}) as 750 and 1879, respectively, whereas the authors of [29] gave the values of 560 and 1530 (differing by about 25% and 19%, respectively). No d–d transitions have been reported in the optical spectra of Fe^{5+} [32] and these authors just estimated the values of B, C and $10Dq$ using the extrapolating method with those values for Cr^{3+} and Mn^{4+} in $SrTiO_3$. Reliability of such an estimation was tested by calculating the EPR parameters, which turned out to be in good agreement with the experimental data [32].

Table 1. Spectroscopic parameters (in cm^{-1}) for Cr^{3+}, Mn^{4+} and Fe^{5+} in $SrTiO_3$.

	Cr^{3+}			Mn^{4+}		Fe^{5+}
B	750	560	662	719	735	800
C	—	—	2587	2839	2816	3050
Dq	1879	1530	1618	1818	1821	2020
Ref.	[28]	[29]	[32]	[21]	[32]	[32]

The overall appearance of the energy level schemes of these systems is determined by the corresponding Tanabe–Sugano diagram [1] (being, more exactly, by its 'strong CF part', since the Dq/B ratio is greater than 2 in every case).

Recently, several papers reporting the *ab initio* calculations of the band structure and elastic constants for pure $SrTiO_3$ were published [34–36]. We shall compare the values of the bulk modulus calculated in this work with those papers.

In section 4 we describe the main theoretical basis for a microscopic analysis of CF effects in the hosts containing 3d ions.

4. Theoretical details

As was mentioned in the introduction, the dependence of $10Dq$ on the 'impurity ion–ligand' chemical bond length R in the vicinity of the equilibrium position can be represented by the following expression [7, 10]:

$$10Dq = \frac{A}{R^n}, \quad (5)$$

where A is a constant. The $10Dq(R)$ functional dependence does not only play a key role in the impurity ion energy levels splitting but influences the EVI between the impurity ion and lattice normal modes [10]. The EVI Hamiltonian in the $^4T_{2g}$ state of a $3d^3$ ion (like the ions considered in the present paper) in the harmonic approximation (if only the a_{1g} and e_g normal vibrational modes of the octahedral complex are considered) can be written in a matrix form as [37]

$$H_{\mathrm{EVI}} = V_{a_{1g}} \begin{pmatrix} Q_{a_{1g}} & 0 & 0 \\ 0 & Q_{a_{1g}} & 0 \\ 0 & 0 & Q_{a_{1g}} \end{pmatrix} + V_{e_g} \begin{pmatrix} \frac{1}{2}Q_{e_{g\theta}} - \frac{\sqrt{3}}{2}Q_{e_{g\varepsilon}} & 0 & 0 \\ 0 & \frac{1}{2}Q_{e_{g\theta}} + \frac{\sqrt{3}}{2}Q_{e_{g\varepsilon}} & 0 \\ 0 & 0 & -Q_{e_{g\theta}} \end{pmatrix}, \quad (6)$$

where $V_{a_{1g}}$, V_{e_g} are the constants of the EVI with the a_{1g} and e_g normal modes, respectively, and $Q_\theta \sim 3z^2–r^2$ and $Q_\varepsilon \sim x^2–y^2$ are the normal coordinates of the e_g Jahn–Teller active mode. $V_{a_{1g}}$ can be expressed in a way similar to $10Dq$ [10]:

$$V_{a_{1g}} = -\frac{nA}{\sqrt{6}R^{n+1}}. \tag{7}$$

Finally, the two EVI constants V_{e_g} and $V_{a_{1g}}$ are related to each other by means of the following simple relation [38]:

$$V_{e_g} = \frac{V_{a_{1g}}}{\sqrt{2}}. \tag{8}$$

One of the most evident experimental observations of EVI is the energetical Stokes' shift $E_S(i)$, which is the difference between the maxima of the lowest absorption and emission bands. If it is caused by the ith normal mode, this shift is defined as [39, 40]

$$E_S(i) = 2S_i\hbar\omega_i = \frac{V_i^2}{M\omega_i^2}, \tag{9}$$

where M is the mass of a single ligand and S_i stands for the non-dimensional Huang–Rhys factor for the ith mode with a frequency ω_i (the vibrational frequencies can be obtained from Raman spectra or analysis of vibronic progressions). It was shown that, for the Cr^{3+} ion in halide crystals, the *total* Stokes' shift E_S arising from the combined effect of both a_{1g} and e_g modes can be written just as a sum of the individual contributions from each mode [39, 40]:

$$E_S = E_S(a_{1g}) + E_S(e_g). \tag{10}$$

We extend this approximation to the isoelectronic Mn^{4+} and Fe^{5+} ions as well. Comparison of the Stokes' shift *calculated* from equations (9) and (10) (based on the actual $10Dq(R)$ dependence) with *experimental* values serves as a good test for the reliability of the calculations.

Since the changes of the interionic distances in a solid are directly related to its elastic constants, one additional application of the $10Dq(R)$ function is straightforward. The local bulk modulus B around an impurity ion can be estimated using the following equation [41]:

$$\left(\frac{\partial 10Dq}{\partial R}\right)_{R=R_0} = -\left(\frac{\partial 10Dq}{\partial P}\right)_{P_0}\frac{3B}{R_0}, \tag{11}$$

where R_0 is the equilibrium interionic distance (usually taken at ambient pressure) and the derivative $\frac{\partial 10Dq}{\partial P}$ shows how the variations of pressure affect the value of $10Dq$. The Grüneisen constant $\gamma(a_{1g})$ (which is defined as $\gamma = -\frac{d(\ln\omega)}{d(\ln V)}$ and shows how the frequencies of vibrational modes change upon changing the volume of the solid) can also be evaluated provided the $10Dq(R)$ function is known. Earlier it was shown [7] that the Stokes' shift for the a_{1g} fully symmetric mode increases with increasing interionic separation:

$$E_S(a_{1g}) = 2S\left(a_{1g}\right)\hbar\omega\left(a_{1g}\right) \propto R^p, \tag{12}$$

where the power p depends on the value of n in the $10Dq(R)$ dependence as

$$p = 9\gamma(a_{1g}) - 2(n+1). \tag{13}$$

Then, if the pressure dependence of $S(a_{1g})$ and $\hbar\omega(a_{1g})$ are known, the lowest possible value of $\gamma(a_{1g})$ can be easily estimated from the condition $p > 0$.

So, indeed the knowledge of the $10Dq(R)$ functional dependence is an important factor for calculating spectroscopic and elastic constants of crystals.

5. Results of calculations and discussion

5.1. Energy level calculations

Since the symmetry of the Ti^{4+} position in $SrTiO_3$ occupied by impurities is O_h, only two non-zero CFP (B_4^0, B_4^4, which are interrelated as $B_4^4 = 5B_4^0$ in the Stevens' normalization) remain in equation (1). Both parameters are of the fourth rank and, as was shown in [42], the crystal lattice sums involved in equation (3) are already converged after extending the summation to the second or the third coordination spheres. To ensure convergence of the crystal lattice sums, we have considered a cluster consisting of 595 ions, which includes the contributions of ions located at the distances up to 15 Å from the impurity ions. This is more than sufficient to get convergence of the fourth-order CFP.

The exchange charge parameters of CF (equation (4)) can be calculated by taking into account the nearest neighbors only (6 oxygen ions in our case), since the overlap integrals with ions from the second and further coordination spheres can be safely neglected. The overlap integrals between the Cr^{3+} (Mn^{4+}, Fe^{5+}) and O^{2-} wavefunctions were calculated numerically using the data from [43, 44]. The calculated overlap integrals (table 2) were approximated by the exponential functions of the interionic distance for the convenience of the following microscopic analysis of the CF strength.

The calculated values of the CFP are collected in table 3. The ECM parameter G for each case was determined by fitting of the $^4T_{2g}$ level to its experimental position in each case; its value also shown in table 3. The electrostatic (equation (3)) and exchange (equation (4)) contributions to CFP are shown separately, to emphasize the importance of the exchange effects. The relative role of the exchange effects monotonically grows up from Cr^{3+} to Fe^{5+}: the $B_{p,S}^k/(B_{p,q}^k + B_{p,S}^k)$ ratios are 0.716, 0.858 and 0.920 for Cr^{3+}, Mn^{4+} and Fe^{5+}, respectively. Thus increase of the oxidation state of the central ion in a complex modifies the electron density distribution and increases delocalization of the ligands' electrons, resulting in an increase of the covalency and enhancement of the nephelauxetic effect in the $Cr^{3+} \rightarrow Mn^{4+} \rightarrow Fe^{5+}$ series [33].

The Hamiltonian (1) with CFP values from table 3 was diagonalized in the basis set spanned by 50 wavefunctions of all eight LS terms of the d^3 electron configuration. Since no fine structure of the experimental absorption bands was reported, the spin–orbit interaction was not considered. The

Table 2. The overlap integrals between the Cr^{3+} (Mn^{4+}, Fe^{5+}) and O^{2-} ions as functions of the interionic separation R ($3.0 < R < 4.0$ atomic units) and the mean values of $\langle r^2\rangle$, $\langle r^4\rangle$ (in au) calculated with wavefunctions from [43, 44].

	Cr^{3+}	Mn^{4+}	Fe^{5+}
$S_s = \langle d0\|s0\rangle$	$-0.901\,11\exp(-0.596\,83R)$	$-0.921\,25\exp(-0.698\,07R)$	$-1.002\,00\exp(-0.811\,19R)$
$S_\sigma = \langle d0\|p0\rangle$	$0.838\,35\exp(-0.641\,18R)$	$0.851\,14\exp(-0.741\,51R)$	$0.900\,92\exp(-0.847\,77R)$
$S_\pi = \langle d1\|p1\rangle$	$1.545\,70\exp(-0.917\,18R)$	$1.464\,40\exp(-1.102\,30R)$	$1.274\,30\exp(-1.09140R)$
$\langle r^2\rangle$	1.434 02	1.098 76	0.880 73
$\langle r^4\rangle$	4.262 82	2.401 20	1.501 54

Table 3. Electrostatic ($B^k_{p,q}$) and exchange ($B^k_{p,S}$) contributions to CFP (in cm^{-1}; Stevens' normalization) for Cr^{3+}, Mn^{4+} and Fe^{5+} in $SrTiO_3$. Total values of the CFP can be obtained using equation (2). The following relation $B^4_4 = 5B^0_4$ holds true (in the Stevens' normalization).

	Cr^{3+}		Mn^{4+}		Fe^{5+}	
	$B^k_{p,q}$	$B^k_{p,S}$	$B^k_{p,q}$	$B^k_{p,S}$	$B^k_{p,q}$	$B^k_{p,S}$
B^0_4	1208	3039	681	4099	426	4877
ECM parameter G	2.608		6.154		15.370	

calculated energy levels (only the lowest ones, located in the experimentally studied spectral range) are shown in table 4, in comparison with corresponding literature data. The energy levels located above the $^4T_{1g}$ (^4F) are not shown in the table, since they are hidden by a strong host absorption [29]. Taking into account that the experimental spectroscopic data from various references are different (tables 1 and 4), agreement between the calculated and observed energy levels is reasonable. It is worthwhile to stress out here that only one parameter of the ECM was allowed to vary freely in our calculations.

It should be pointed out that the ^2E_g level is located well below the spin-quartet $^4T_{2g}$, which is a clear manifestation of a strong CF in all considered cases.

5.2. Dependence of 10Dq on distance in $SrTiO_3$ doped with Cr^{3+}, Mn^{4+} and Fe^{5+}

For an ion with three d electrons in a cubic CF the value of $10Dq$ is exactly equal to the energy of the first excited spin-quartet $^4T_{2g}$ [1]. After calculating the energy level schemes of all three considered ions at the equilibrium distance of $R_0 = 1.9526$ Å, we have performed similar calculations of CFP and energy level splitting for other distances, greater and smaller than R_0 with a step of 1% in the range $R_0 \pm 5\%$. Such a range of variation covers well all the effects of the lattice relaxation (unavoidable when impurity ions are incorporated into a crystal) and pressure variation. The values of the ECM parameter G were not changed, since they provide good agreement with available experimental data. Table 5 summarizes the numerical results of these calculations, whereas figure 2 visualizes them. The calculated $10Dq$ values are indicated in figure 2 by symbols (different for each considered chemical element); the fitting lines (the power laws) and their equations are also given in the figure. The quality of fitting was determined by the correlation coefficient R^2, whose values are also shown in the figure. The closer this value is to unity, the better is the fit. In all cases, the correlation coefficient was not less than 0.999, so the fitting results are reliable.

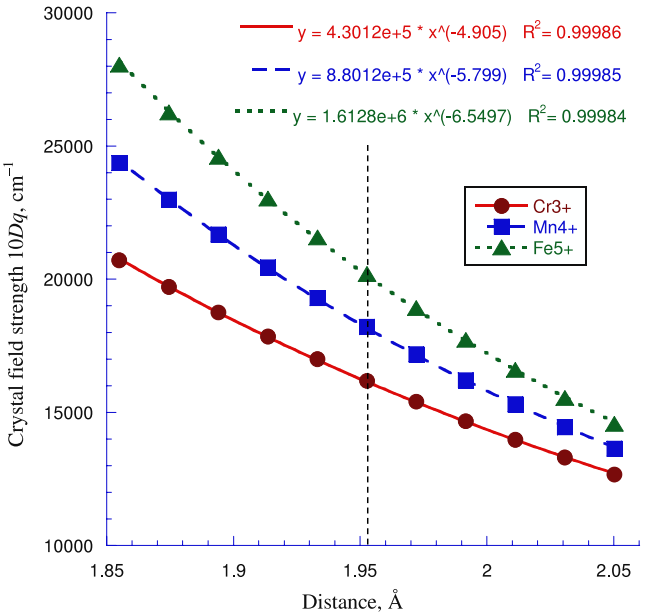

Figure 2. Dependence of the CF strength $10Dq$ on distance for Cr^{3+} (circles), Mn^{4+} (squares) and Fe^{5+} (triangles) in $SrTiO_3$. The vertical dashed line corresponds to the equilibrium separation of 1.9526 Å between impurities and oxygen ions.

Both values of n and constant A in equation (5) are increasing with increasing impurity ion oxidation state, i.e. in the $Cr^{3+} \rightarrow Mn^{4+} \rightarrow Fe^{5+}$ direction. In all three considered systems, the value of n differs from 5 and, obviously, this difference comes from the second term in equation (2) (since the first term from equation (2), being taken separately, immediately would yield $n = 5$). To reveal the roles played by both terms in the $10Dq(R)$ dependence, we have plotted the dependences of the Coulomb point charge (equation (3)) and exchange (equation (4)) contributions to CFP (figure 3). Again, the calculated values were fitted by the power laws and their equations are shown in figure 3, as well as in table 5. The plots of the Coulomb point charge contributions are shown merely to illustrate that their magnitudes are several times smaller than their exchange charge counterparts.

As predicted by the point charge model, the Coulomb point charge contributions behave as A/R^5, but the A values decrease with increasing impurity ion charge. Such a trend can be explained by the decrease of the $\langle r^4\rangle$ values when going from Cr^{3+} to Fe^{5+} (table 2). The ratios $A(Cr^{3+}):A(Mn^{4+}):A(Fe^{5+})$ are equal to the ratios $\langle r^4\rangle(Cr^{3+}):\langle r^4\rangle(Mn^{4+}):\langle r^4\rangle(Fe^{5+})$.

Table 4. The lowest calculated (this work) energy levels (in cm^{-1}) for Cr^{3+}, Mn^{4+} and Fe^{5+} in $SrTiO_3$ in comparison with available experimental data. The values of the Racah parameters (in cm^{-1}) for each ion are also given. No d–d transitions were observed in $SrTiO_3$:Fe^{5+} [32].

	Cr^{3+} ($B = 662$, $C = 2581$)		Mn^{4+} ($B = 735$, $C = 2812$)		Fe^{5+} ($B = 800$, $C = 3050$)	
O_h group irreps.	Calculated	Observed	Calculated	Observed	Calculated	Observed
$^4A_{2g}$	0	0	0	0	0	—
^2E_g	12 598	12 594 [29]	13 831	13 827 [29]	15 034	—
$^2T_{1g}$	13 207	—	14 508	—	15 767	—
$^4T_{2g}$	16 181	16 260 [29]	18 210	17 300 [29]	20 201	—
		16180 [32]		18210 [21]		—
$^2T_{2g}$	19 105	—	21 026	—	22 900	—
$^4T_{1g}$	22 763	21 277 [29]	25 543	25 400 [29]	28 221	—

Table 5. The calculated values (in cm^{-1}) of total CF strength $10Dq$ (defined as the $^4T_{2g}$–$^4A_{2g}$ energy gap) for Cr^{3+}, Mn^{4+} and Fe^{5+} in $SrTiO_3$. The point charge contribution of the point charge model (PCC PCM) and exchange charge contributions of the exchange charge model (ECC ECM) are given separately. Approximating functions are also shown. In these equations R is in Å and the calculated result is the energy in cm^{-1}.

	Cr^{3+}			Mn^{4+}			Fe^{5+}		
Distance to the oxygen ions (Å)	PCC PCM	ECC ECM	Total	PCC PCM	ECC ECM	Total	PCC PCM	ECC ECM	Total
$R_0 - 5\%$	5948	14 755	20 703	3 352	21 012	24 364	2 095	25 964	28 059
$R_0 - 4\%$	5645	14 059	19 704	3 180	19 802	22 982	1 988	24 283	26 271
$R_0 - 3\%$	5360	13 395	18 755	3 020	18 661	21 681	1 888	22 711	24 599
$R_0 - 2\%$	5092	12 761	17 853	2 869	17 585	20 454	1 793	21 241	23 034
$R_0 - 1\%$	4839	12 156	16 995	2 727	16 572	19 299	1 704	19 866	21 570
$R_0 = 1.9526$ Å	4602	11 578	16 182	2 593	15 617	18 210	1 621	18 580	20201
$R_0 + 1\%$	4379	11 027	15 406	2468	14 716	17 184	1543	17 377	18 920
$R_0 + 2\%$	4169	10 501	14 670	2349	13 868	16 217	1468	16 253	17 721
$R_0 + 3\%$	3970	10 000	13 970	2237	13 068	15 305	1398	15 201	16 609
$R_0 + 4\%$	3783	9 522	13 305	2131	12 315	14 446	1332	14 218	15 550
$R_0 + 5\%$	3606	9 066	12 672	2032	11 605	13 637	1270	13 298	14 568
Approximating functions	$\frac{130\,650}{R^5}$	$\frac{299\,810}{R^{4.867}}$	$\frac{430\,120}{R^{4.905}}$	$\frac{73\,615}{R^5}$	$\frac{824\,800}{R^{5.9323}}$	$\frac{880\,120}{R^{5.799}}$	$\frac{46\,019}{R^5}$	$\frac{1624\,000}{R^{6.6856}}$	$\frac{1612\,800}{R^{6.5497}}$

The exchange charge contributions behave in the opposite way: they increase with increasing impurity ion charge, which is directly related to increase of the overlap integrals and overall enhancement of the covalent effects in the $Cr^{3+} \rightarrow Mn^{4+} \rightarrow Fe^{5+}$ series, as was also shown in [33].

It can also be seen from figures 2 and 3 that the Fe^{5+} dependences are steeper than those of Mn^{4+}, which, in turn, is steeper than those of Cr^{3+}. This circumstance will have a very important influence on the EVI parameters and Jahn–Teller stabilization energies (since these quantities are related to the derivative of the $10Dq(R)$, following equations (7) and (8)), as will be shown in section 5.3.

5.3. Electron-vibrational interaction in $SrTiO_3$ doped with Cr^{3+}, Mn^{4+} and Fe^{5+}

Table 6 shows the results of calculations of the EVI constants, Stokes' shifts and Huang–Rhys parameters performed using the above-obtained analytical expressions for $10Dq$. Required frequencies of the a_{1g} and e_g normal modes were taken from [45]. Comparison of the calculated results for all three ions shows that the EVI is enhanced when increasing the central ion oxidation state, resulting in an increase of both Huang–Rhys factors and Stokes' shifts.

After the values of the Huang–Rhys factors are estimated, evaluations of the Jahn–Teller stabilization energy E_{JT} become straightforward: $E_{JT} = S_{e_g}\hbar\omega_{e_g}$. The corresponding values are also given in table 6.

To visualize the potential energy surfaces in the $^4T_{2g}$ state (which are split as a result of the Jahn–Teller effect and have the shape of a tricorn) and estimate the magnitudes of distortions of the oxygen octahedra around impurities in $SrTiO_3$, we follow the procedure described in detail in [46, 47].

The potential energy surface in terms of the normal coordinates displacements $\Delta Q_{a_{1g}}$, ΔQ_{e_g} can be written as

$$V = \tfrac{1}{2}K_{a_{1g}}\left(\Delta Q_{a_{1g}} - \Delta Q_{a_{1g},eq}\right)^2 + \tfrac{1}{2}K_{e_g}\left(\Delta Q_{e_g} - \Delta Q_{e_g,eq}\right)^2 \quad (14)$$

with the magnitudes of the normal displacements defined as ($i = a_{1g}, e_g$)

$$|\Delta Q_i|_{eq} = \left[\frac{2S_i\hbar\omega_i}{K_i}\right]^{1/2} \quad (15)$$

and the force constants K_i estimated by the F–G matrix method [48]; their numerical values are given in table 6. The magnitude of the e_g mode is always negative, as was shown in [49, 50]. As will be shown below, the values of $|\Delta Q_i|_{eq}$ are

Table 6. Calculated (this work) values of the EVI constants, Huang–Rhys parameters, total Stokes' shifts, Jahn–Teller energies and chemical bond changes for Cr^{3+}, Mn^{4+} and Fe^{5+} in $SrTiO_3$. Frequencies of the a_{1g} and e_g modes are 887 and 545 cm^{-1}, respectively [45]. E_S was calculated using equation (10). $R_0 = 1.9526$ Å.

	Force constants		EVI constants		Huang–Rhys factors				Normal coordinates magnitudes (Å)		Chemical bond lengths changes (Å)	
	$K_{a_{1g}}$ (N m^{-1})	K_{e_g} (N m^{-1})	$V_{a_{1g}}$ (N)[a]	V_{e_g} (N)[a]	$S_{a_{1g}}$	S_{e_g}	Stokes' shift E_S (cm^{-1})	Jahn–Teller energy E_{JT} (cm^{-1})	$\Delta Q_{a_{1g}}$	ΔQ_{e_g}	Δx, Δy	Δz
Cr^{3+}	567	214	-3.29×10^{-9} (-166)	-2.32×10^{-9} (-117)	0.41	0.89	1706	485	0.050	−0.095	0.048	−0.034
Mn^{4+}	574	217	-4.37×10^{-9} (-220)	-3.09×10^{-9} (-156)	0.73	1.58	3020	861	0.067	−0.126	0.064	−0.045
Fe^{5+}	577	218	-5.48×10^{-9} (-276)	-3.87×10^{-9} (-195)	1.15	2.48	4737	1352	0.084	−0.157	0.080	−0.056

[a] The value in cm^{-1} pm^{-1} is given in parentheses.

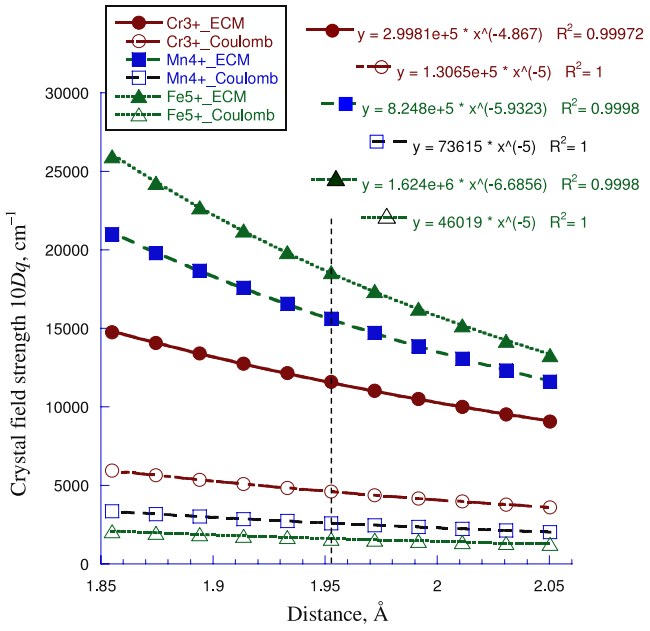

Figure 3. Dependence of the point charge (empty symbols; Cr^{3+}—circles, Mn^{4+}—squares, Fe^{5+}—triangles) and the exchange charge (filled symbols) contributions to the CF strength $10Dq$ in $SrTiO_3$. The vertical dashed line is the same as in figure 2.

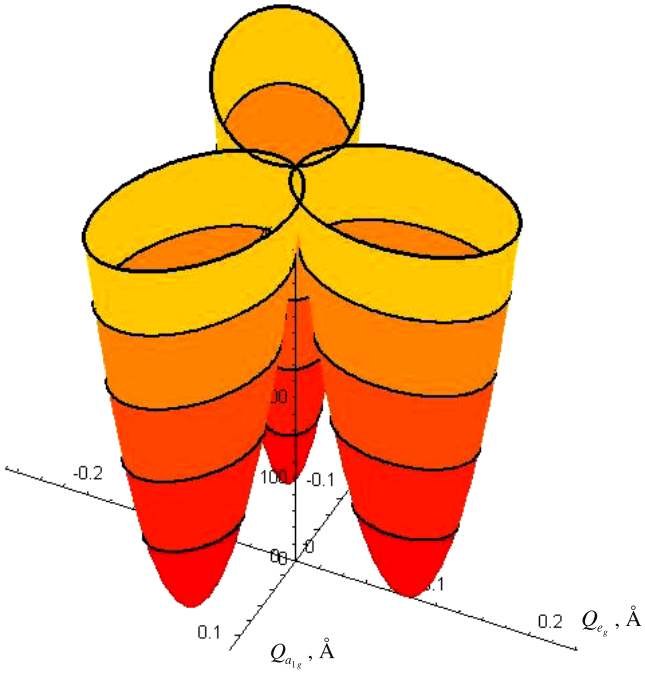

Figure 4. The $^4T_{2g}$ state potential energy surface for Cr^{3+} in $SrTiO_3$ as a function of the normal coordinate displacements. The energies of the individual contours are (in cm^{-1}, from bottom to top) 100, 200, 300, 400 and 485.

merely needed to convert the combined effect of several normal modes into the chemical bond changes.

It should be noted here that the coordinate system in the $Q_{e_g\theta}$, $Q_{e_g\varepsilon}$ space (these are the two components of the doubly degenerate e_g mode) can always be chosen in such a way that the potential minimum of the considered $^4T_{2g}$ component (any one from ξ, η, ζ) lies on the Q_θ axis (this means no distortion takes place along the Q_ε axis). Then it is possible to consider the $|\Delta Q_{e_g}|_{eq}$ values as corresponding to $|\Delta Q_{e_{g\theta}}|_{eq}$, whereas the $|\Delta Q_{e_{g\varepsilon}}|_{eq}$ values are zero. This assumption simplifies the visual representation of the obtained results.

Figures 4 and 5 visualize the $^4T_{2g}$ potential energy surface and its cross section for Cr^{3+} in $SrTiO_3$. Three sheets of the potential energy surface intersect at the (0, 0, E_{JT}) point, and the value of the potential energy at this point corresponds to the Jahn–Teller stabilization energy for the considered $[CrO_6]^{9-}$ complex in $SrTiO_3$, which is about 485 cm^{-1}. The potential energy plots for the two remaining ions are very similar and are not shown here for the sake of brevity. Instead, the numerical estimations of the Jahn–Teller energies and corresponding deformations for the $[MnO_6]^{8-}$ and $[FeO_6]^{7-}$ complexes are given in table 6. Finally, the magnitudes of the normal displacements are converted into the chemical bond changes Δx, Δy, Δz by using the following matrix [49]:

$$\begin{pmatrix} \Delta x \\ \Delta y \\ \Delta z \end{pmatrix} = \frac{1}{2} \begin{pmatrix} \sqrt{\frac{2}{3}} & -\sqrt{\frac{1}{3}} & -1 \\ \sqrt{\frac{2}{3}} & -\sqrt{\frac{1}{3}} & 1 \\ \sqrt{\frac{2}{3}} & \sqrt{\frac{4}{3}} & 0 \end{pmatrix} \begin{pmatrix} \Delta Q_{a_{1g}} \\ \Delta Q_{e_g\theta} \\ \Delta Q_{e_g\varepsilon} \end{pmatrix}. \qquad (16)$$

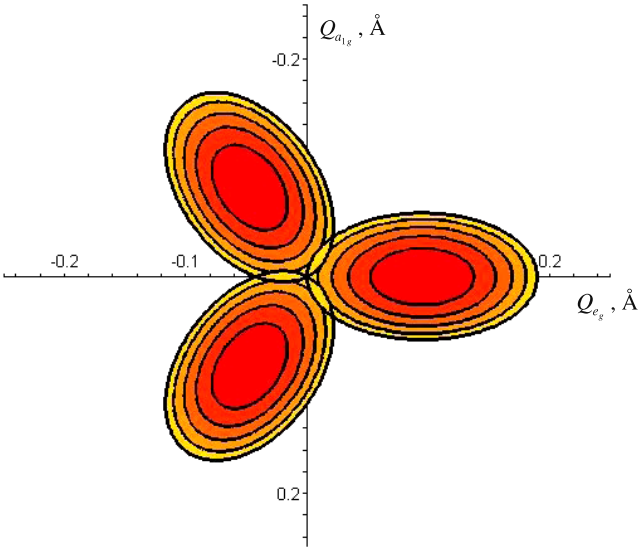

Figure 5. The top view of the $^4T_{2g}$ state potential energy surface for Cr^{3+} in $SrTiO_3$. The energies of the individual contours are (in cm^{-1}) 100, 200, 300, 400 and 485. The point of intersection of all three sheets (indicated by a black circle at the origin of the reference system in the figure) corresponds to the value of the Jahn–Teller energy of 485 cm^{-1}.

The corresponding changes Δx, Δy, Δz (these are simply the changes of the oxygen octahedron around impurities) are given in table 6. As seen from these results, all $[CrO_6]^{9-}$, $[MnO_6]^{8-}$ and $[FeO_6]^{7-}$ complexes undergo an equatorial expansion in the xy plane and an axial compression along the z axis; the magnitude of these deformations increases with increasing central ion electrical charge.

Increase of the EVI and force constants implies that, to produce equal changes in the interionic distances and vibration frequencies in all these three systems, an external force (or applied pressure) should be increased when changing the dopants from Cr to Mn and then to Fe in $SrTiO_3$.

5.4. Estimations of the elastic constants (bulk modulus and Grüneisen parameter) for $SrTiO_3$ doped with Cr^{3+}, Mn^{4+} and Fe^{5+}

It was demonstrated in [7] that the Huang–Rhys factor $S(a_{1g})$ for the fully symmetric mode increases with increasing R, which means that $S(a_{1g})$ decreases when the applied pressure increases. Such a behavior of $S(a_{1g})$ would be possible if the value of p from equation (13) is positive. Then the lowest estimation of the Grüneisen constant $\gamma(a_{1g})$ can be obtained in a straightforward manner by solving inequality $p > 0$ (provided the distance dependence of $10Dq$ is known). Using the values of n from table 5, the lowest estimations of $\gamma(a_{1g})$ are as follows: 1.31 for the $[CrO_6]^{9-}$ complex, 1.51 for the $[MnO_6]^{8-}$ complex and 1.68 for the $[FeO_6]^{7-}$ complex. The lowest estimates of $\gamma(a_{1g})$ decrease with decreasing n; in other words, the frequency of vibrations more slightly depends on the changes of interatomic distances in cases of smaller n. This can be interpreted such that the variations of the interionic separations are not strongly 'felt' by neighbors, which has another manifestation in a form of weaker covalency in the $[CrO_6]^{9-}$ complex, as compared with the $[MnO_6]^{8-}$ and $[FeO_6]^{7-}$ complexes, in agreement with the results of ECM calculations.

Equation (11) can be used to estimate the bulk modulus B and a local compressibility $\chi = 1/B$ around an impurity. This, however, implies knowledge of the pressure dependence of $10Dq$. Unfortunately, we did not find any results of high-pressure studies of the optical properties for the title systems, except for the pressure dependence of the EPR spectra of Cr^{3+} in $SrTiO_3$ reported in [28]. These data are analogues to the measurements of the pressure dependence of the CF strength, since the g shift measured in the EPR experiments can be expressed in terms of $10Dq$ for Cr^{3+} as follows [1]:

$$\Delta g = g - g_0 = -\frac{8\lambda}{30Dq}, \tag{17}$$

with $g_0 = 2.0023$ and λ being the one-electron spin–orbit interaction (SO) constant, $\lambda = \frac{\zeta}{2S}$, with S being the total spin of a particular electron configuration ($S = 3/2$ in our case) and ζ is the 'many-electron' SO constant for a considered ion in a particular spin state. It should be noted here that this constant for an ion in a crystal is somewhat lower than in a free state. The typical values of the SO constant ζ for Cr^{3+} in crystals are about 220–230 cm^{-1} [3, 4], and then the one-electron SO constant λ is readily estimated to be about 75–80 cm^{-1}. It is easy to get the pressure dependence of the CF strength $10Dq$ from equation (17) if the pressure dependence of Δg is known.

Using the experimental data on the dependence of Δg from hydrostatic pressure (approximated by a straight line in [28], whose equation can be written as $g = 1.9789 + 6.6718 \times 10^{-5}P$, where P is the pressure in kbar) and the one-electron SO constant estimated by those authors for Cr^{3+} 55 cm^{-1} (which is actually significantly underestimated), we obtained for $SrTiO_3$:Cr^{3+} the value of $B = 148$ GPa. It can be already compared in principle with the previously reported experimental value of 179 GPa [51] and the calculated values from first-principles methods, distributed in a very wide range from 169 to 252 GPa [34–36].

Nevertheless, we noticed two circumstances which contribute to the discrepancy between the experimental value of B and our calculations:

(i) the value of the one-electron SO constant suggested in [28] is too small;
(ii) the last experimental point (figure 6, [28]) corresponding to the measurements at 10 kbar deviates considerably from the straight line, in comparison with others.

So, we eliminated the 10 kbar experimental value of Δg; with this assumption the linear approximation of g is then $g = 1.979 + 4.7477 \times 10^{-5}P$. Using the value of the one-electron SO constant as 70 cm^{-1} (which is more realistic), we obtained $B = 162$ GPa, considerably closer to the experimental value than the first estimation.

With such a value of the bulk modulus, the compressibility for the $[CrO_6]^{9-}$ unit in $SrTiO_3$ is $\chi_{calc} = 1/B_{calc} = 6.17 \times 10^{-3}$ $kbar^{-1}$, which is not far from the experimental value $\chi_{exp} = 1/B_{exp} = 5.59 \times 10^{-3}$ $kbar^{-1}$ [51].

6. Conclusion

A systematic microscopic study of the crystal field effects upon the energy levels and electron-vibrational interaction for Cr^{3+}, Mn^{4+} and Fe^{5+} at octahedral positions in cubic $SrTiO_3$ was performed in the present paper. A systematic change of the impurity ions allowed us to consider how the optical and dynamical properties of an impurity center depend on the impurity ion. For the first time, the exchange charge model of a crystal field was applied to determine the dependence of the crystal field strength $10Dq$ on interionic distance R. It was shown that for all considered crystals $10Dq$ depends on R as $1/R^n$, with $n = 4.9050$, 5.7990 and 6.5497 for Cr^{3+}, Mn^{4+} and Fe^{5+}, respectively. The deviations of these values from the value $n = 5$ (predicted by the simple point charge model of a crystal field) is explained by the covalent and exchange effects; the contribution of these effects to the total crystal field strength was considered separately.

The $10Dq$ functions obtained as a result of our calculations were used for estimations of the electron-vibrational constants, force constants, Huang–Rhys parameters, Stokes' shifts, Jahn–Teller stabilization energies, deformations of the considered octahedral complexes and Grüneisen constant $\gamma(a_{1g})$ for all the above-mentioned systems and local compressibility around the $[CrO_6]^{9-}$ complex in $SrTiO_3$. It was shown that the electron-vibrational interaction is considerably enhanced with increase of the central ion oxidation state. The results of this work can be readily applied for analysis of the pressure dependences of the absorption and luminescence spectra of the studied materials.

Reasonably good agreement between the calculated and experimental values (when available) confirms the validity of the obtained results and the developed approach itself, which can be applied to other crystals with 3d ions as well.

References

[1] Sugano S, Tanabe Y and Kamimura H 1970 *Multiplets of Transition-Metal Ions in Crystals* (New York: Academic)
[2] Ballhausen C J 1962 *Introduction to Ligand Field Theory* (New York: McGraw-Hill)
[3] Henderson B and Imbush G F 2006 *Optical Spectroscopy of Inorganic Solids* (Oxford: Clarendon)
[4] Powell R C 1998 *Physics of Solid-State Laser Materials* (Berlin: Springer)
[5] Tanabe Y and Sugano S 1954 *J. Phys. Soc. Japan* **9** 766
[6] Sugano S and Tanabe Y 1958 *J. Phys. Soc. Japan* **13** 880
[7] Moreno M, Barriuso M T and Aramburu J A 1992 *J. Phys.: Condens. Matter* **4** 9481
[8] Moreno M, Barriuso M T and Aramburu J A 1994 *Int. J. Quantum Chem.* **52** 829
[9] Wissing K, Aramburu J A, Barriuso M T and Moreno M 1998 *Solid State Commun.* **108** 1001
[10] Moreno M, Barriuso M T, Aramburu J A, García-Fernández P and García-Lastra J M 2006 *J. Phys.: Condens. Matter* **18** R315
[11] Moreno M, Aramburu J A and Barriuso M T 2004 *Struct. Bonding* **106** 127
[12] Bray K L 2001 *Top. Curr. Chem.* **213** 1
[13] Kaminska A, Dmochowski J E, Suchocki A, Garcia-Sole J, Jaque F and Arizmendi L 1999 *Phys. Rev.* B **60** 7707
[14] Galanciak D, Grinberg M, Gryk W, Kobyakov S, Suchocki A, Boulon G and Brenier A 2005 *J. Phys.: Condens. Matter* **17** 7185
[15] Grinberg M and Suchocki A 2007 *J. Lumin.* **125** 97
[16] Brik M G and Ogasawara K 2006 *Phys. Rev.* B **74** 045105
[17] García-Lastra J M, Moreno M and Barriuso M T 2008 *J. Chem. Phys.* **128** 144708
[18] García-Lastra J M, Barriuso M T, Aramburu J A and Moreno M 2008 *Phys. Rev.* B **78** 085117
[19] García-Lastra J M, Barriuso M T, Aramburu J A and Moreno M 2008 *Appl. Magn. Reson.* **34** 149
[20] Malkin B Z 1987 *Spectroscopy of Solids Containing Rare-Earth Ions* ed A A Kaplyanskii and B M Macfarlane (Amsterdam: North-Holland) pp 33–50
[21] Bryknar Z, Trepakov V, Potucek Z and Jastrabic L 2000 *J. Lumin.* **87–89** 605
[22] Trepakov V A, Kudyk I B, Kapphan S E, Savinov M E, Pashkin A, Jasrtrabik L, Tkach A, Vilarinho P M and Kholkin A L 2003 *J. Lumin.* **102/103** 536
[23] La Mattina F, Bednorz J G, Alvarado F, Shengelaya A and Keller H 2008 *Appl. Phys. Lett.* **93** 022102
[24] Liu J W, Chen G, Li Z H and Zhang Z G 2006 *J. Solid State Chem.* **179** 3704
[25] Tkach A, Vilarinho P M, Kholkin A L, Pashkin A, Veljko S and Petzelt J 2006 *Phys. Rev.* B **73** 104113
[26] Ryu H, Singh B K, Bartwal K S, Brik M G and Kityk I V 2008 *Acta Mater.* **56** 358
[27] Mitchell R H, Chakhmouradian A R and Woodward P M 2000 *Phys. Chem. Miner. (Germany)* **27** 583
[28] Rimai L, Deutsch T and Silverman B D 1964 *Phys. Rev.* **133** A1123
[29] Stokowski S E and Schawlow A L 1969 *Phys. Rev.* **178** 457
[30] Grabner L 1969 *Phys. Rev.* **177** 1315
[31] Trepakov V A, Vikhnin V S, Kapphan S, Jastrabik L, Licher J and Syrnikov P P 2000 *J. Lumin.* **87–89** 1126
[32] Zheng W C and Wu X X 2005 *J. Phys. Chem. Solids* **66** 1701
[33] Brik M G and Avram N M 2006 *J. Phys. Chem. Solids* **67** 1599
[34] Piskunov S, Zhukovski Yu F, Kotomin E A and Shunin Yu N 2000 *Comput. Modell. New Techol.* **4** 7
[35] Piskunov S, Heifets E, Eglitis R I and Borstel G 2004 *Comput. Mater. Sci.* **29** 165
[36] Shein I R, Kozhevnikov V L and Ivanovskii A L 2008 *Solid State Sci.* **10** 217
[37] Sturge M D 1967 *Solid State Phys.* **20** 91
[38] Wissing K and Degen J 1998 *Mol. Phys.* **95** 51
[39] Woods A M, Sinkovits R S, Charpie J C, Huang W L, Bartram R H and Rossi A R 1993 *J. Phys. Chem. Solids* **54** 543
[40] Barriuso M T, Aramburu J A and Moreno M 1994 *Phys. Status Solidi* b **196** 193
[41] Hernández D, Rodríguez F, Moreno M and Güdel H U 1999 *Physica* B **265** 186
[42] Brik M G, Avram N M, Avram C N, Rudowicz C, Yeung Y Y and Gnutek P 2007 *J. Alloys Compounds* **432** 61
[43] Clementi E and Roetti C 1974 *At. Data Nucl. Data Tables* **14** 177
[44] Eremin M V 1989 *Spectroscopy of Crystals* (Leningrad: Nauka) pp 30–44 (in Russian)
[45] Tinte S and Shirley E L 2008 *J. Phys.: Condens. Matter* **20** 365221
[46] Wenger O S and Güdel H U 2001 *J. Chem. Phys.* **114** 5832
[47] Avram C N, Brik M G, Tanaka I and Avram N M 2005 *Physica* B **355** 164
[48] Venkateswarlu K and Sundaram S 1956 *Phys. Chem. Neue Folge* **9** 174
[49] Solomon E I and McClure D S 1974 *Phys. Rev.* B **9** 4690
[50] Wilson R B and Solomon E I 1978 *Inorg. Chem.* **17** 1729
[51] Hellwege K H and Hellwege A M 1969 *Ferroelectrics and Related Substances* (*Landolt-Bornstein, New Series Group III* vol 3) (Berlin: Springer)